Materials Physics and Mechanics 29 (2016) 116-124 Received: October 26, 2016

LOCALIZED WAVES IN CARBON NANO-STRUCTURES WITH CONNECTED AND DISCONNECTED OPEN WAVEGUIDES

S.A. Nazarov[1,2,3*], K. Ruotsalainen[4], P. Uusitalo[4]

[1]Institute of Problems of Mechanical Engineering RAS, Bolshoj pr. 61, V.O., St. Petersburg, 199178, Russia

[2]Peter the Great St. Petersburg Polytechnic University,

Polytechnicheskaya ul. 29, St. Petersburg, 195251, Russia

[3]Saint-Petersburg State University, Universitetsky pr. 28, Peterhof, St. Petersburg, 198504, Russia

[4]University of Oulu, Applied and Computational Mathematics, Oulu, 90014, Finland

*e-mail: srgnazarov@yahoo.co.uk

Abstract. A hexagonal lattice of quantum waveguides is considered with thickening or thinning of ligaments, which form open waveguides in the periodic nano-structure. Propagation of localized waves along the open connected and disconnected waveguides is studied and nodes in the lattice are indicated that support trapped modes with the exponential decay in all directions.

1. Problem setting

The graph G^0 in the plane $\mathbb{R}^2$ (see Fig. 1a) for a hexagonal one dimensional structure consisting of vertices and unit straight segments, edges, is expressed as a union of the shifts $g^0(\tau)$, $\tau = (\tau_1, \tau_2)$, $\tau_j \in \mathbb{Z} = \{0, \pm 1, \pm 2, \dots\}$, of the fundamental cell g^0 entered into the parallelogram $\mathbb{P}$ (shaded in Fig. 1a) defined by the vectors $e_\pm = \left(3/2\,, \pm\sqrt{3}/2\right)$. Angles between each three edges emerging from a vertex are $2\pi/3$. We consider two types of the "fat" structures in Fig. 1b, and 2a and b,

$$G^h = \{x = (x_1, x_2) : \mathrm{dist}(x, G^0) < h/2\},\ G_H^h = \left(G^h \setminus L_1^h\right) \cup L_H^h, \qquad (1)$$

where L_H^h is an open waveguide, either connected or disconnected. To obtain L_H^h, one chooses a subgraph L^0 in G^0 which can be a path as in Fig. 2a, or disruptive as in Fig. 2b. Then, L_H^h is a tubular hH-neighborhood of L^0. In the case $H < 1$, we observe thinning of ligaments in $L_1^h \subset G^h$ and thickening while $H > 1$.

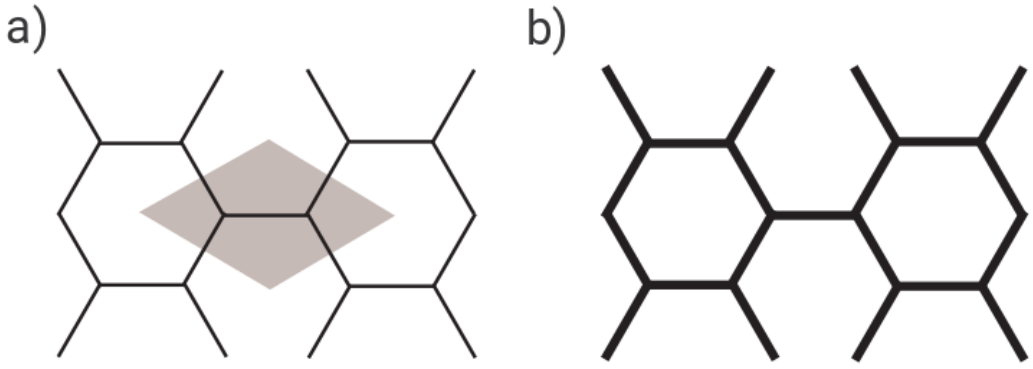

Fig. 1. The hexagonal graph G^0 and the fattened lattice G^h.

In many publications, cf. [1-3] and the review papers [4, 5], the classical Pauling model [6] is employed to simulate the quantum waveguides on the thin lattice G^h (the Dirichlet condition on the boundary). However, as was proved in [7], on the base of general results [8], mathematically well-grounded one-dimensional model on the graph G^0 involves the Dirichlet condition at all vertices instead of the Kirchhoff transmission conditions in the Pauling model which is justified for a lattice of acoustic waveguides (the Neumann condition), see [9, 10]. It should be mentioned that a one-dimensional model of the lattice G_R^h with the disks of radius hR centered at each vertex of the graph G^0 can obtain various types of transmission conditions under the limit passage $h \to +0$, see [10] for the Neumann case and [11] for the Dirichlet case.

We consider the spectral Dirichlet problem for the Laplace operator Δ

$$-\Delta u_H^h(x) = \lambda_H^h u_H^h(x), \ x \in G_H^h, \tag{2}$$

$$u_H^h(x) = 0, \qquad x \in \partial G_H^h, \tag{3}$$

which is associated [12, §10] with a positive self-adjoint operator A_H^h in Lebesgue space $L^2\left(G_H^h\right)$. In [7], we have examined the spectrum σ_1^h of the operator A_1^h of the problem (2), (3) in the homogeneous lattice $G^h = G_1^h$, that is for $H = 1$. A result [7] related to the low-frequency range of σ_1^h demonstrates that the interval $(0, h^{-2}\pi^2)$ includes two spectral bands β_1^h and β_2^h which are situated near the point $h^{-2}\mu_1^1$ and have lengths $\mathcal{O}\left(e^{-\delta_1^1/h}\right)$; see Section 2 for the positive numbers μ_1^1 and $\delta_1^1 > 0$. Actually, β_1^h and β_2^h give rise only one passing zone because these bands coincide with each other due to the geometrical symmetry of the cell. The very small length of the passing zone $\beta_1^h = \beta_2^h$ for waves in the lattice assures the existence of two wide spectral gaps, stopping zones, below and above these bands.

The main goal of our paper is to demonstrate that the deformations of the lattice G^h which are depicted in Fig. 2, as bold lines and are called open waveguides, see [13] and compare [14, 15], bring additional short passing zones to the low-frequency range. In other words, rows of defects in a periodic medium, indeed, may provoke waves propagating along them and decaying at a distance from them. Although such phenomenon has been discussed in the physical literature, cf. [16], our result is the first one derived rigorously. Moreover, in certain situation we are able to indicate trapped modes, i.e., eigenfunctions of the problem (2), (3) in G_H^h which decay in all directions and are localized in the vicinity of a single node (marked with ⊙ in Fig. 2a).

The very reason for the above-mentioned modification of the spectrum is the fact that the operator A_H^h with $H \neq 1$ is not a compact perturbation of the operator A_1^h, cf. [12, §9]. This natural observation was translated in [13] into a general mathematical tool detecting the changes of the essential spectrum of periodic media due to introduction of rows of foreign inclusions.

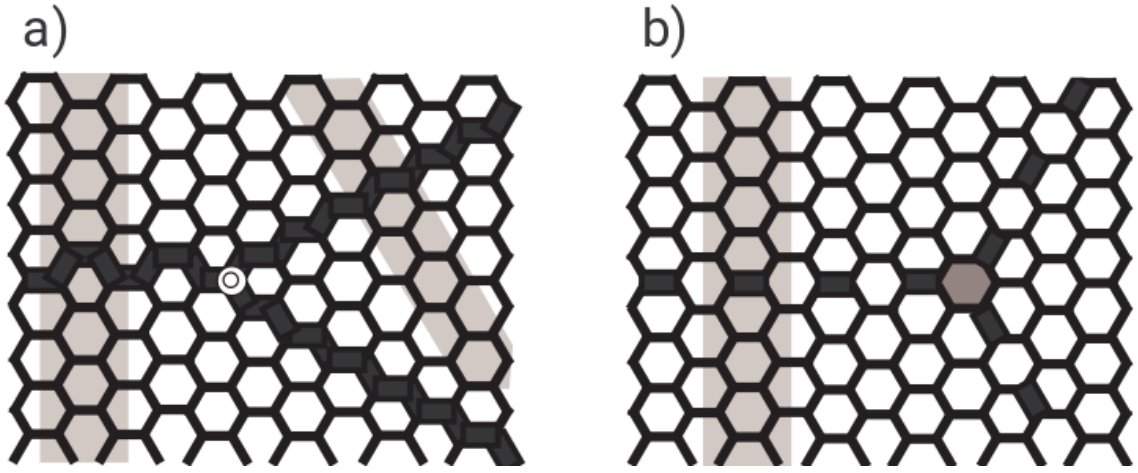

Fig. 2. The connected (a) and disconnected (b) open waveguides.

2. The discrete spectrum of infinite tripod waveguides

Let us consider the Dirichlet problem

$$-\Delta w^H(\xi) = \mu^H w^H(\xi),\ \xi \in Y_H^1, \tag{4}$$

$$w^H(\xi) = 0, \qquad \xi \in \partial Y_H^1. \tag{5}$$

The infinite waveguide Y_H^h is composed from three pointed semi-strips, see Fig. 3a. The horizontal strip S_H^0 is of width H and the tilted ones $S_h^{\pm}$ of width h. Mid-lines of S_H^0 and $S_h^{\pm}$ meet each other at the coordinate origin $\xi = 0$ and the angles between them are $2\pi/3$. The junction Y_H^1, in particular with $H = 1$, is obtained from G_H^h by the coordinate dilation

$$x \mapsto \xi = h^{-1}(x - \mathcal{O}) \tag{6}$$

and the formal passage to $h = 0$; here, $\mathcal{O}$ is a vertex of the graph G^0.

The continuous spectrum Σ_H^{co} of the problem (4), (5) is the semi-axis $[\mu_\dagger(1,H), +\infty)$ with the cut-off value $\mu_\dagger(1,H) = \pi^2 \min\{1, H^{-2}\}$. It was verified in [7] that the discrete spectrum Σ_1^{di} consists of the only point $\mu_1^1 \in (0, \pi^2)$. It is also known, see e.g. [17], that the V-shaped waveguide shaded in Fig. 3c has a non-empty discrete spectrum in $(0, \pi^2)$ and, hence the comparison principle [12, Theorem 10.2.2] assures the existence of an eigenvalue in Σ_H^{di} for $H < 1$. The same principle proves that the total multiplicity $\#\Sigma_H^{di}$ is one because $\#\Sigma_H^{di} \le \#\Sigma_1^{di} = 1$ for $H < 1$.

The case $H > 1$ is slightly more complicated because the growth of H leads to a decrease of the cut-off value $\mu_\dagger(1,H)$ in the waveguide Y_H^1. However, in the same way as in [19] it is possible to find $H_* > 1$ such that $\#\Sigma_H^{di} = 1$ when

$$H \in (0, H_*) \tag{7}$$

The discrete spectrum is empty for $H \ge H_*$. In what follows we vary the width H within the interval (7) and denote the corresponding isolated eigenvalue by $\mu_H^1 \in \left(0, \mu_\dagger(1,H)\right)$.

Remark. A result in [20] demonstrates that the problem (4), (5) in the waveguide $Y_{H_*}^1$ with the critical width H_* has a bounded solution at the threshold spectral parameter $\mu = \mu_\dagger(1, H_*)$. As was shown, see [7] and [11] for hexagonal lattices, this peculiar feature of the tripod causes a change of transmission conditions at the vertices of the graph G^0 modeling the lattice.

The coordinate change $\xi \mapsto H^{-1}\xi$ reveals the only point $\mu_H^H = H^{-2}\mu_1^1$ in the discrete spectrum of the waveguide Y_H^H composed of three congruent tapered strips of width $H \ne 1$. The same transformation converts Y_1^H into $Y_{1/H}^1$ and, thus, $\mu_1^H = H^{-2}\mu_{1/H}^1$. To keep the conclusion on the single eigenvalue we assume in this case that $H \in (H_*^{-1}, +\infty)$. The eigenfunction W_H^h of the problem (4), (5) in Y_H^h corresponding to the above-mentioned eigenvalue $\mu_H^h \in \left(0, \mu_\dagger(h,H)\right)$ has the exponential decay at infinity

$$W_H^h(\xi) = \mathcal{O}\left(e^{-\delta_H^h |\xi|}\right),\ \delta_H^h = \sqrt{\pi^2 - \left(\mu_H^h\right)^2} > 0. \tag{8}$$

We normalize this function in Lebesgue space $L^2\left(Y_H^h\right)$.

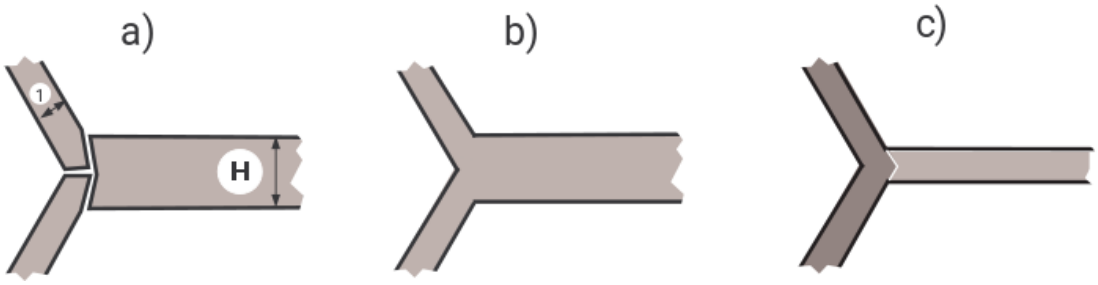

Fig. 3. The Y-shaped waveguide.

3. The low-frequency range of the spectrum in the homogeneous lattice G^h

The periodicity cell $g^h = G^h \cap \mathbb{P}$ contains five rectangles g_0^h, $g_{l\pm}^h$ and $g_{r\pm}^h$, where l and r mean left and right. The one-dimensional periodicity cell $g^0 = G^0 \cap \mathbb{P}$ consists of two vertices $\mathcal{O}_l$, $\mathcal{O}_r$ and five segments $g_0^0 = \{z_0 : z_0 \in (-½, ½)\}$, $g_{l\pm}^0 = \{z_\mp : \pm z_\mp \in (0, ½)\}$, $g_{r\pm}^0 = \{z_\pm : \pm z_\pm \in (0, ½)\}$ where z_α, $\alpha = 0, \pm$, is the local coordinate, the longitudinal coordinate in $g_{l-\alpha}^h$, $g_{r\alpha}^h$, while the transversal coordinate is denoted by $y_\alpha \in (-h/2\,, h/2)$.

In the framework of the Floquet-Bloch-Gelfand theory, cf. [21-23], the Gelfand transform converts the problem (2), (3) in the homogeneous lattice G^h into the spectral problem

$$-\Delta U^h(x;\theta) = \Lambda(\theta) U^h(x;\theta),\ x \in g^h, \tag{9}$$

$$U^h(x;\theta) = 0,\ x \in \partial g^h \setminus t^h, \tag{10}$$

with the quasi-periodicity conditions

$$U^h(x;\theta)|_{z_\pm = ½} = e^{i\theta_\pm} U^h(x;\theta)|_{z_\pm = -½}\,, \tag{11}$$

$$\partial_{z_\pm} U^h(x;\theta)|_{z_\pm = ½} = e^{i\theta_\pm} \partial_{z_\pm} U^h(x;\theta)|_{z_\pm = -½}. \tag{12}$$

on the segments of truncation

$$t_{l\pm}^h = \{x \in \partial g^h : z_\mp = ½\}, t_{r\pm}^h = \{x \in \partial g^h : z_\pm = ½\}, \tag{13}$$

the union of which is denoted in (10) by t^h. Here, $\theta = (\theta_+, \theta_-) \in [-\pi, \pi]^2$ is the dual Gelfand variable or the Floquet parameter.

The spectrum of the problem (9)-(12) is discrete and forms the monotone unbounded sequence

$$0 < \Lambda_1^h(\theta) \le \Lambda_2^h(\theta) \le \cdots \le \Lambda_n^h(\theta) \le \cdots \longrightarrow +\infty, \tag{14}$$

where multiplicity of eigenvalues is taken into account. The functions $[-\pi, \pi]^2 \ni \theta \longmapsto \Lambda_n^h(\theta)$ are continuous and 2π-periodic in $\theta_\pm$. Hence, they determine spectral bands, i.e., the compact connected segments

$$\beta_n^h = \{\Lambda_n^h(\theta) : \theta \in [-\pi, \pi]^2\}. \tag{15}$$

The spectrum of the operator A_1^h or of the problem (2), (3) in $G^h = G_1^h$ is the union of the segments (15):

$$\sigma_1^h = \bigcup_{n\in\mathbb{N}} \beta_n^h\,,\ \mathbb{N} = \{1,2,3,\dots\}. \tag{16}$$

In the paper [7] we have proved that, first, $\Lambda_3^h(\theta) > h^{-2}\pi^2$, and second, the endpoints of the bands $\beta_j^h = \left[\beta_{j-}^h, \beta_{j+}^h\right], j = 1,2$, admit the asymptotics

$$\beta_{j\pm}^h = h^{-2}\left(\mu_1^1 \pm \mathcal{O}\left(e^{-2\delta_1/h}\right)\right),\ \delta_1 = \sqrt{\pi^2 - \mu_1^1}. \tag{17}$$

In other words, the low-frequency range $(0, h^{-2}\pi^2]$ of the spectrum (16) includes only two spectral bands which coincide and have exponentially small length in the vicinity of the rescaled eigenvalue $h^{-2}\mu_1^1$ of the problem (4), (5) in Y_1^1.

4. The disconnected open waveguide

In view of the periodicity lost, we cannot use the Gelfand transform in the distorted lattice G_H^h, see (1) and Fig. 2. To investigate the spectrum σ_H^h of the problem (2), (3) in the lattice drawn in Fig. 2b and containing the intermitted open waveguide L_H^h, we employ an approach in [17] and consider the left half $G_{H-}^h = G_H^h \cap \mathbb{R}_-^2$ of the lattice G_H^h while ignoring the periodicity failure in the right half $G_{H+}^h = G_H^h \cap \mathbb{R}_+^2$ and extending G_{H-}^h periodically along the x_1-axis; here $\mathbb{R}_\pm^2 = \{x = (x_1, x_2) : \pm x_1 > 0\}$. Then we apply the partial Gelfand transform

$$u(x) \longmapsto U(x;\vartheta) = \frac{1}{\sqrt{2\pi}} \sum_{j\in\mathbb{Z}} e^{i\vartheta 3j} u(x_1 + 3j, x_2)$$

with the dual variable $\vartheta \in (-\pi/3\,, \pi/3)$. Notice that the above-mentioned extension of G_{H+}^h produces a 3-periodic domain in the x_1-direction. Finally, we arrive at the spectral problem

$$-\Delta U(x;\vartheta) = \Lambda(\vartheta) U(x;\vartheta),\ x \in \Pi_H^h, \tag{18}$$

$$U(x;\vartheta) = 0,\ x \in \partial\Pi_H^h \setminus \left(T_{H+}^h \cup T_{H-}^h\right) \tag{19}$$

in the infinite vertical truss $\Pi_H^h = \left\{x: |x_1| < \frac{3}{2}, (x_1 - 3N, x_2) \in G_{H+}^h\right\}$ (this domain is independent of $N \in \mathbb{N}$ and enters the shaded strip in Fig. 2b with the quasi-periodicity conditions at the truncation sets $T_{H\pm}^h = \left\{x: x_1 = \pm\frac{3}{2}, (x_1 - 3N, x_2) \in G_{H+}^h\right\}$

$$U(x;\vartheta)|_{T_{H-}^h} = e^{i3\vartheta} U(x;\vartheta)|_{T_{H+}^h}, \tag{20}$$

$$\frac{\partial U}{\partial x_1}(x;\vartheta)|_{T_{H-}^h} = e^{i3\vartheta} \frac{\partial U}{\partial x_1}(x;\vartheta)|_{T_{H+}^h}. \tag{21}$$

Here, $\Lambda(\vartheta)$ is a new notation for the spectral parameter.

The variational form of the problem (18)-(21) reads

$$(\nabla U, \nabla V)_{\Pi_H^h} = \Lambda(\vartheta)(U,V)_{\Pi_H^h} \quad \forall V \in H_{0\vartheta}^1\left(\Pi_H^h\right) \tag{22}$$

and gives rise [12; §10] to a positive definite self-adjoint operator $A_H^h(\vartheta)$ in the Lebesgue space $L^2\left(\Pi_H^h\right)$. In (22), $H_{0\vartheta}^1\left(\Pi_H^h\right)$ is the Sobolev space of functions verifying the Dirichlet condition (19) and the stable quasi-periodicity condition (20). According to [24], [25; §3] and [17], the essential spectrum $\Sigma_{H,es}^h(\vartheta)$ of the operator $A_H^h(\vartheta)$, that is of the problem (22) or (18)-(21), includes the set

$$\cup_{n\in\mathbb{N}}\{\Lambda_n^h(3\vartheta, \theta_-): \theta_- \in [-\pi, \pi]\} \tag{23}$$

constructed from eigenvalues (14) but also may get the discrete spectrum $\Sigma_{H,di}^h(\vartheta)$ below $\Sigma_{H,es}^h(\vartheta)$ or inside spectral gaps in (23).

The truss Π_H^h has two nodes with center points $\mathcal{O}^\pm = (\pm½, 0)$, see Fig. 4a.

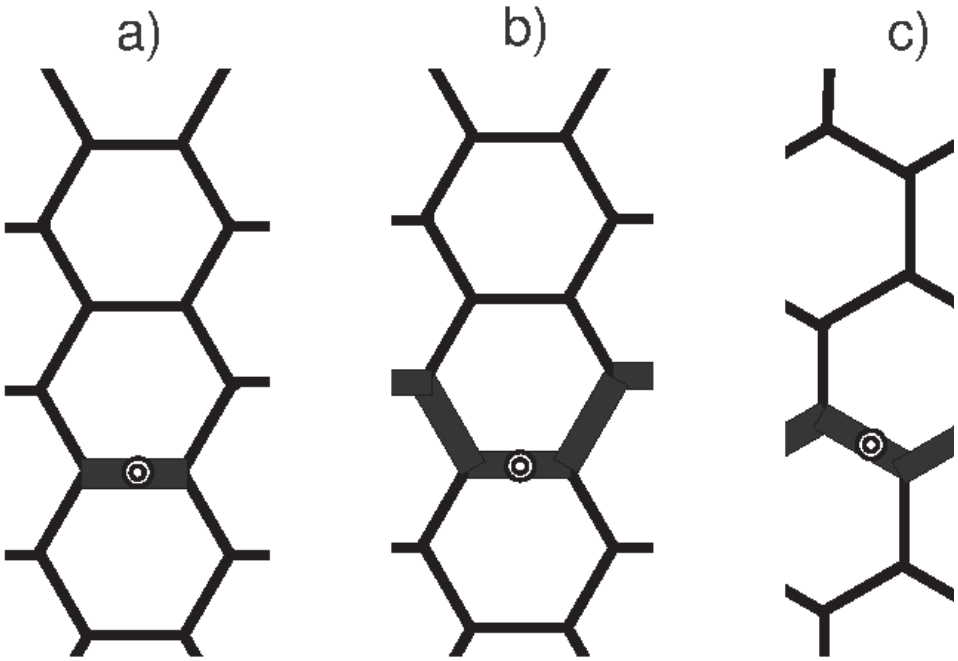

Fig. 4. The periodicity truss Π_H^h in the disconnected waveguide (a) and in the connected waveguide (b and c).

By the coordinate dilation (6), these nodes turn into the infinite tripod waveguide Y_H^1 and its mirror reflection. The number $h^{-2}\mu_H^1$ and the functions $W_{H\pm}^h(x) = \chi^h(x - \mathcal{O}^\pm)w_H^1(\xi^\pm)$ with an appropriate cut-off function χ^h, see Section 6, are perfect approximations for the eigenvalue $\Lambda_\pm^h(\vartheta)$ and the eigenfunction $U_\pm^h(x;\vartheta)$ of the problem (18)-(21). According to (8), the couple $\left\{h^{-2}\mu_H^1, W_{H\pm}^h\right\}$ leaves the exponentially small discrepancy in h in the differential equation (18) and satisfies the relations (19)-(21) in full. In Section 6 we will demonstrate that this evidence provides the approximation estimates

$$\left|\Lambda_{\pm}^{h}(\vartheta) - h^{-2}\mu_H^1\right| \le ch^{-5/2}e^{-\delta_H^1/h}, \left|\Lambda_{\pm}^{h}(\vartheta) - h^{-2}\mu_H^1\right| \le ch^{-5/2}e^{-\delta_H^1/h}, \quad (24)$$

$$\left\|\nabla\left(U_{\pm}^{h}(\cdot;\vartheta) - W_{H\pm}^1\right);\ L^2(\Pi_H^h)\right\| + h^{-1}\left\|U_{\pm}^{h}(\cdot;\vartheta) - W_{H\pm}^1;\ L^2(\Pi_H^h)\right\| \le\ ch^{-3/2}e^{-\delta_H^1/h}. \quad (25)$$

We underline several facts. First, the truss Π_H^h is symmetric with respect to the x_2-axis, i.e.

$$\Pi_H^h = \left\{x: (-x_1, x_2)\ \in \Pi_H^h\right\}, \quad (26)$$

and, thus, $\Lambda_+^h(\vartheta) = \Lambda_-^h(\vartheta)$ and the spectral band

$$B_H^h = \left\{\Lambda_{\pm}^{h}(\vartheta): \vartheta \in \left[-\frac{\pi}{3}, \frac{\pi}{3}\right]\right\} \quad (27)$$

is the same for plus and minus. Second, the value μ_H^1 is clearly independent of the Floquet parameter ϑ so that the estimate (24) proves that the band (27) has length $\mathcal{O}\left(e^{-\delta_H^1/h}\right)$. Third, in the case $H \in (1, H_*)$ we have $\mu_H^1 < \mu_1^1$ and, therefore, the band (27) is situated below the essential spectrum (16) of the homogeneous lattice G^h while, for $H < 1$, the band B_H^1 lies inside the spectral gap between the bands $\beta_1^h = \beta_2^h$ and β_3^h, see (15), because of the inequality $\mu_H^1 > \mu_1^1$ and the asymptotic formulas (17) and (24). Finally, two inclined intermitted open waveguides in the right half G_{H+}^h of the lattice G_H^h in Fig. 2b give rise to the spectral problem (18)-(21) in the same truss Π_H^h (only the rotation of the coordinate system is needed). In this way, multiplicity of the continuous spectrum in B_H^h is six. Clearly, the band (27) generated simultaneously by three semi-infinite open waveguides L_H^h in G_H^h is absent in the spectrum (16) of G^h. We will discuss consequential wave processes in Section 7.

5. The connected open waveguide

The essential spectrum of the problem (2), (3) in the lattice G_H^h (see Fig. 2a), is investigated along the same scheme as in Section 4. However, some modifications are needed and we list them below.

1° The problem (18)-(21) serving for the open waveguide $L_H^h \cap \mathbb{R}_-^2$ is posed in the truss Π_H^h (it enters the shaded strip in Fig. 2a) with a different configuration of perturbed ligaments (compare Fig. 4b and a). There are four nodes with center $\mathcal{O}_{\pm}^1 = (\pm 1/2\,, 0)$ and $\mathcal{O}_{\pm}^2 = \left(\pm 1, \sqrt{3}/2\right)$ which become into the infinite tripod waveguide Y_1^H after the coordinate dilation (6). The corresponding eigenvalue $\mu_1^H = H^{-2}\mu_{1/H}^1$ belongs to $(0, \mu_1^1)$ and (μ_1^1, π^2) in the cases $H \in (1, +\infty)$ and $H \in (H_*^{-1}, 1)$, respectively.

2° The asymptotic formulas for four eigenvalues $\Lambda_{H\pm}^{hj}(\vartheta), j = 1,2$, look as follows:

$$\left|\Lambda_{H\pm}^{hj}(\vartheta) - h^{-2}\mu_1^H\right| \le ch^{-5/2}e^{-\delta_1^H/h}. \quad (28)$$

Due to the mirror symmetry with respect to the x_2-axis, we have $\Lambda_{H+}^{hj}(\vartheta) = \Lambda_{H-}^{hj}(-\vartheta)$, cf. Section 4. Furthermore, the change $x \longmapsto \left(x_1 - \frac{3}{2}, -x_2 + \frac{\sqrt{3}}{2}\right)$ does not affect the shape of L_{H-}^1 and therefore, $\Lambda_{H\pm}^{h1}(\vartheta) = \Lambda_{H\mp}^{h2}(\vartheta + \pi/3)$. In other words, formula (27) with $\Lambda_{H\pm}^{hj}(\vartheta)$, $j = 1,2$, gives only one spectral band B_H^h with multiplicity four of the continuous spectrum in it.

3° The truss generated by both inclined open waveguides of L_{H+}^h in Fig. 2a, obtains a different set of perturbed ligaments, see Fig. 4c. We still observe two nodes with centers $\mathbb{O}_{\pm}^1 = \left(\pm\frac{\sqrt{3}}{4}, \mp\frac{1}{4}\right)$ which convert into Y_1^H after the coordinate dilation. Although the asymptotic analysis and the estimate (28) remain valid, the new spectral band $\mathbb{B}_H^h$ with multiplicity four does not coincide with B_H^h from 2° and this leads to the peculiar features of propagation of localized waves as discussed in Section 7.

6. The discrete spectrum and trapped modes in G_H^h

The triple open waveguide G_H^h has a specific node with the center $x = (0,0)$ marked by $\odot$ in Fig. 2a. Namely, the coordinate dilation (6) transforms it into the waveguide Y_H^H with three

outlets of equal width H. The eigenvalue in the discrete spectrum of Y_H^H satisfies the relations

$$H^{-2}\mu_1^1 = \mu_H^H < \mu_1^H < \mu_1^1 \text{ for } H \in (1, H_*), \tag{29}$$

$$H^{-2}\mu_1^1 = \mu_H^H > \mu_1^H > \mu_1^1 \text{ for } H \in (H_*^{-1}, 1). \tag{30}$$

Thus, in the case (29) the point $h^{-2}\mu_H^H$ stays below the essential spectrum of the lattice G_H^h but in the case (30) it belongs to the spectral gap between the bands β_3^h and B_H^h, $\mathbb{B}_H^h$ described above.

Let us outline the standard scheme to prove the existence of an eigenvalue $\Lambda_{H\odot}^h$ in the discrete spectrum of the problem (2), (3). The Hilbert space $\mathcal{H}_H^h = H_0^1(G_H^h)$ consisting of functions in the Sobolev space $H^1(G_H^h)$ which enjoy the Dirichlet condition (3), is equipped with the scalar product

$$\langle u_H^h, v_H^h\rangle = \left(\nabla u_H^h, \nabla v_H^h\right)_{G_H^h} + h^{-2}\left(u_H^h, v_H^h\right)_{G_H^h}, \tag{31}$$

where ∇=grad and $(\,,\,)_{G_H^h}$ is the natural scalar product in the Lebesgue space $L^2(G_H^h)$. Instead of the unbounded operator A_H^h in Section 1, the identity

$$\langle \mathcal{A}_H^h u_H^h, v_H^h\rangle = \left(u_H^h, v_H^h\right)_{G_H^h} \quad \forall u_H^h, v_H^h \in \mathcal{H}_H^h \tag{32}$$

gives us the positive definite symmetric and continuous, therefore, self-adjoint operator $\mathcal{A}_H^h$ in $\mathcal{H}_H^h$.

By the definitions (31) and (32), the variational formulation

$$\left(\nabla u_H^h, \nabla v_H^h\right)_{G_H^h} = \lambda_H^h\left(u_H^h, v_H^h\right)_{G_H^h} \quad \forall v_H^h \in \mathcal{H}_H^h \tag{33}$$

of the problem (2), (3) becomes the abstract equation $\mathcal{A}_H^h u_H^h = \kappa_H^h u_H^h$ in $\mathcal{H}_H^h$ with a new spectral parameter

$$\kappa_H^h = \left(h^{-2} + \lambda_H^h\right)^{-1}. \tag{34}$$

The norm of $\mathcal{A}_H^h$ is smaller than one and, hence, its spectrum $\mathcal{S}_H^h$ belongs to [0,1]. The relations (29) and (30) demonstrate that a Ch^2-neighborhood of the point

$$\mathcal{K}_H^h = h^2(1 + \mu_H^H)^{-1} \tag{35}$$

is free of the essential spectrum $\mathcal{S}_H^{h,es}$ of $\mathcal{A}_H^h$. However, the well-known formula, see e.g. [12; §6.1],

$$dist\left(\mathcal{K}_H^h, \mathcal{S}_H^h\right) = \left\|\left(\mathcal{A}_H^h - \mathcal{K}_H^h\right)^{-1};\ \mathcal{H}_H^h \longrightarrow \mathcal{H}_H^h\right\|^{-1}$$

shows that, under the condition

$$\left\|\mathcal{A}_H^h \mathcal{U}_H^h - \mathcal{K}_H^h \mathcal{U}_H^h; \mathcal{H}_H^h\right\| \le Ch^{3/2}e^{-\delta/h}\left\|\mathcal{U}_H^h; \mathcal{H}_H^h\right\|,\ \delta > 0, \tag{36}$$

there exists an eigenvalue $\kappa_{H\odot}^h$ of $\mathcal{A}_H^h$ such that

$$\left|\kappa_{H\odot}^h - \mathcal{K}_H^h\right| \le ch^{3/2}e^{-\delta/h} \implies \left|\lambda_{H\odot}^h - h^{-2}\mu_1^1\right| < ch^{-5/2}e^{-\delta/h}. \tag{37}$$

The last estimate follows from (35).

Let us build a function $\mathcal{U}_H^h$ which satisfies (36), namely

$$\mathcal{U}_H^h(x) = \chi^h(x) w_H^H(h^{-1}x), \tag{38}$$

where χ^h is a smooth cutoff function,

$$\chi^h(x) = 1 \text{ for } |x| < 1 - 4h,\ \chi^h(x) = 0 \text{ for } |x| > 1 - 2h. \tag{39}$$

We easily derive the estimate

$$\left\|\mathcal{U}_H^h; \mathcal{H}_H^h\right\|^2 \ge 2h(1 + \mu_H^H), \tag{40}$$

where formulas $\left\|w_H^h; L^2(Y_H^H)\right\| = 1$ and $mes_2 supp\,(\chi^h) \ge 2h$ were taken into account. Furthermore, using a definition of the norm in Hilbert space, we derive

$$\left\|\mathcal{A}_H^h \mathcal{U}_H^h - \mathcal{K}_H^h \mathcal{U}_H^h; \mathcal{H}_H^h\right\| = sup\left|\langle \mathcal{A}_H^h \mathcal{U}_H^h - \mathcal{K}_H^h \mathcal{U}_H^h, \mathcal{V}_H^h\rangle\right| =$$

$$h^2(1 + \mu_H^H)^{-1} sup\left|\left(\nabla \mathcal{U}_H^h, \nabla \mathcal{V}_H^h\right)_{G_H^h} - h^{-2}\mu_H^H\left(\mathcal{U}_H^h, \mathcal{V}_H^h\right)_{G_H^h}\right| =$$

$$h^2(1 + \mu_H^H)^{-1} sup\left|\left(\Delta \mathcal{U}_H^h + h^{-2}\mu_H^H \mathcal{U}_H^h, \mathcal{V}_H^h\right)_{G_H^h}\right|. \tag{41}$$

where supremum is computed over all $\mathcal{V}_H^h \in \mathcal{H}_H^h$ such that $\|\mathcal{V}_H^h; \mathcal{H}_H^h\| = 1$ and, in particular, $\|\mathcal{V}_H^h; L^2(G_H^h)\| \le h$. The relations (31), (35) and the Green formula were applied in the calculation of (41). We write

$$\Delta\mathcal{U}_H^h + h^{-2}\mu_H^H\mathcal{U}_H^h = (\Delta + h^{-2}\mu_H^H)\mathcal{U}_H^h + [\Delta, \chi^h]\mathcal{U}_H^h$$

and observe that the first term on the right vanishes because of the equation (4) under the coordinate change (6). The modulo of the commutator

$$[\Delta, \chi^h]\mathcal{U}_H^h(x) = 2\nabla\chi^h(x)\cdot\nabla w_H^H(h^{-1}x) + w_H^H(h^{-1}x)\Delta\chi^h(x) \tag{42}$$

does not exceed $ch^{-2}e^{-\delta_H^H/h}$ by the virtue of the decay rate in (8) and the equality $\nabla\chi^h = 0$ for $|x| \le 1 - 2h$, see (39). Thus, the quantity (41) is bounded by $ch^2e^{-\delta_H^H/h}$ and together with (40) confirms the relation (36) and the desired estimate (37).

The eigenfunction $u_{H\odot}^h \in H_0^1(G_H^h)$, a trapped mode, which corresponds to the eigenvalue $\lambda_{H\odot}^h$ indicated in (37), is strictly localized in the vicinity of the node marked with $\odot$ in Fig. 2a, and decays at the very high ($h^{-1} \gg 1$ is a big parameter) rate $\mathcal{O}(e^{-\delta|x|/h})$ at a distance $|x|$ from this node. Indeed, an estimate of type (25) that accompanies our calculations (38), (40)-(42) can be converted, cf. [26], into the following weighted estimate:

$$\|e^{\delta|x|/h}\nabla(u_{H\odot}^h - \mathcal{U}_H^h); L^2(G_H^h)\| + h^{-1}\|e^{\delta|x|/h}(u_{H\odot}^h - \mathcal{U}_H^h);\ L^2(G_H^h)\| \le ce^{-\delta/h}$$

with some $\delta > 0$.

The above-discussed trapped mode $u_{H\odot}^h$ is born by the only node $\odot$ in Fig. 2a, thick ($H > 1$) or thin ($H < 1$) in three directions. The authors do not know if a trapped mode can appear as a result of interaction of two or several nodes, e.g., the vertices of the deeply shaded hexagon in Fig. 2b.

7. Propagation of localized waves along open waveguides

For the lattice G_H^h in Fig. 2b, the continuous spectrum in the band (27), absent in the essential spectrum (16) of the homogeneous lattice G^h, has multiplicity six and is generated by three couples of the incoming and outgoing waves which travel along three branches of L_H^h backwards and towards infinity, respectively. This classification of the localized waves and their normalization can be made on the basis of the Mandelstam (energy) principle [27], see also [28; §1], [25; §5] and [29]. Moreover, the scattering matrix of size 3×3 can be determined in order to describe wave propagation along the whole open waveguide L_H^h. This matrix, as usual, cf. [20, 29], is unitary and symmetric (not necessarily Hermitean) but, owing to the evident rotational symmetry in Fig. 2b, it does not change under the cyclic permutation of columns and rows. In this way, the energy of a wave coming along L_{H-}^1 from infinity is divided between the reflected outgoing wave and, in equal parts, between two waves outgoing along the inclined branches of L_{H+}^h.

The symmetry is clearly broken in Fig. 2a. Hence, the scattering 3×3-matrix defined in the same way but for $\lambda_H^h \in B_H^h \cap \mathbb{B}_H^h$, loses invariance with respect to cyclic permutations so that the energy distribution between branches in L_{H+}^h is no longer equal. Furthermore, in the case $\lambda_H^h \in B_H^h \setminus \mathbb{B}_H^h \ne \emptyset$ wave processes do not occur in L_{H+}^h (both branches are "closed" for waves) and, therefore, an incoming wave along L_{H-}^h is reflected completely but the scattering matrix of size 2×2 still exists because although the waveguide L_{H-}^h is closed, both branches in L_{H+}^h are open.

All the above-mentioned waves are localized near the open waveguides L_H^h and decay exponentially at a distance from them. At the same time, one observes other sort of localization in the estimate (25), namely the wave propagations realizes as strong oscillation of nodes in the connected or disconnected path L_H^h but its ligaments stay in relative rest.

Acknowledgements
This research was supported by Russian Science Foundation (Grant 14-29-00199).

References

[1] P. Kuchment, O. Post // *Communications in Mathematical Physics* **275(3)** (2007) 805.
[2] E. Korotyaev, I. Lobanov // *Annales Henri Poincare* **8(6)** (2007) 1151.
[3] I.Y. Popov, A.N. Skorynina, I.V. Blinova // *Journal of Mathematical Physics* **55(3)** (2014) 033504.
[4] P. Kuchment // *Waves in Random Media* **12(1)** (2002) R1.
[5] P. Kuchment // *Waves in Random Media* **14(1)** (2004) 107.
[6] L. Pauling // *The Journal of Chemical Physics* **4** (1936) 673.
[7] S.A. Nazarov, K. Ruotsalainen, P. Uusitalo // *Comptes Rendus Mecanique* **343** (2015) 360.
[8] D. Grieser // *Proceedings of the London Mathematical Society* **97(3)** (2008) 718.
[9] P. Kuchment, H. Zeng // *Contemporary Mathematics* **387** (2003) 199.
[10] P. Exner, O. Post // *Journal of Geometry and Physics* **54(1)** (2005) 77.
[11] S.A. Nazarov, K. Ruotsalainen, P. Uusitalo // *Materials Physics and Mechanics* **29(2)** (2016) 107.
[12] M.S. Birman, M.Z. Solomyak, *Spectral Theory and Self-Adjoint Operators in Hilbert Space* (Reidel, Dordrecth, 1987).
[13] G. Cardone, S.A. Nazarov, J. Taskinen // *Journal of Functional Analysis* **269(8)** (2015) 2328
[14] A.-S. Bonnet-Ben Dhia, G. Dakhia, B. Goursaud, C. Hazard, L. Chorfi // *SIAM Journal of Applied Mathematics* **70(3)** (2009) 677.
[15] A.-S- Bonnet-Ben Dhia, B. Goursaud, C. Hazard // *SIAM Journal of Applied Mathematics* **71(6)** (2001) 2048.
[16] J.P. Carini, J.T. Longergan, D.P Murdock, *Binding and scattering in two-dimensional systems: Application to quantum wires, waveguides and photonic crystals* (Springer-Verlag, Berlin, 1999).
[17] S.A Nazarov // *St. Petersburg Mathematical Journal* **23(2)** (2011) 351.
[18] D.S. Jones // *Mathematical Proceedings of the Cambridge Philosophical Society* **49** (1953) 668.
[19] S.A. Nazarov // *Journal of Mathematical Sciences* **196(3)** (2013) 346.
[20] S.A. Nazarov // *Theoretical and Mathematical Physics* **167(2)** (2011) 606.
[21] P. Kuchment // *Russian Mathematical Surveys* **37(4)** (1982) 1.
[22] M.M Skriganov // *Proceedings of the Steklov Institute of Mathematics* **171** (1987) 1.
[23] P. Kuchment, *Floquet theory for partial differential equations* (Basel, Birchäuser, 1993).
[24] S.A. Nazarov // *Mathematics of the USSR-Izvestiya* **18(1)** (1982) 89.
[25] S.A. Nazarov, B.A Plamenevskii, *Elliptic problems in domains with piecewise smooth boundaries* (Walter de Gruyter, Berlin, 1994).
[26] S.A. Nazarov // *Computational Mathematics and Mathematical Physics* **54(5)** (2014) 1261
[27] L.I. Mandelstam, *Lectures on Optics, the Theory of Relativity, and Quantum Mechanics* (Izd. AN SSSR, Moscow, 1947). (In Russian).
[28] I.I. Vorovich, V.A Babeshko, *Dynamical Mixed Problems of Elasticity for Nonclassical Domains* (Nauka, Moscow, 1979). (In Russian).
[29] S.A. Nazarov // *Sbornik: Mathematics* **205(7**) (2014) 953.